

## Computed cross section for resonant charge transfer in $\text{Ba}^+ + \text{Ba}$ collisions

Stanley J. Sramek

*Department of Physics, University of Nebraska, Lincoln, Nebraska 68588*

(Received 31 December 1979)

The cross section for the resonant electron transfer process  $\text{Ba}^+ + \text{Ba} \rightarrow \text{Ba} + \text{Ba}^+$  is calculated for collision energies up to 800 keV. Energy curves for the  ${}^2\Sigma_u^+$  and  ${}^2\Sigma_g^+$  molecular states are first obtained using the multiconfiguration valence-bond method. The cross section is then obtained from the energy curves using the two-state impact parameter version of the perturbed stationary states method. The differential cross section is obtained using the eikonal method. Total cross-section values up to approximately  $200\pi a_0^2$  are obtained. At low energies the total cross section exhibits rapid, strong interference oscillations of the type commonly considered to be associated with local extrema in the two-state energy difference. The differential cross-section results clearly show that impact-parameter-dependent structural details of the transfer probability are not directly observable.

### I. INTRODUCTION

In recent years there has been a considerable growth of interest in charge-transfer collisions between atoms and ions. Many theoretical and experimental studies of such processes have been performed. Most of this work, however, has involved lighter atoms and ions; comparatively little effort has been devoted to studying charge transfer between heavy species. In particular, few *ab initio* theoretical studies of such heavy systems have been performed.

This author and his associates have already calculated cross sections for the nonresonant charge-transfer process  $\text{Ba}^+ + \text{Ba}^+ \rightarrow \text{Ba} + \text{Ba}^{2+}$ , for collision energies of several hundred keV.<sup>1</sup> Knowledge of such cross sections is essential to the development of the heavy ion heating approach to inertial confinement fusion.<sup>2</sup> This earlier calculation also provided important insights regarding the qualitative nature of the transient phenomena, occurring during the collision, that lead to charge transfer.

The earlier work has now been extended to a treatment of the resonant charge-transfer process  $\text{Ba}^+ + \text{Ba} \rightarrow \text{Ba} + \text{Ba}^+$ . This new calculation complements the previous work and provides further insight concerning the nature of heavy ion charge-transfer processes in general. These two treatments, of systems involving Ba species, probably illustrate several of the most important physical characteristics of charge-transfer processes common to nearly all heavy ion systems.

The theory used in the present calculation is described in Sec. II. The numerical results are presented and discussed in Sec. III. A short comparative discussion of the resonant charge-transfer results and of the earlier nonresonant results is conducted in Sec. IV.

### II. THEORY

The first step in this calculation is to obtain a set of electronic energies and eigenfunctions for the molecular system  $\text{Ba}_2^+$ , as functions of the distance between the two Ba nuclei. That is, approximate solutions to the eigenvalue problem

$$H(\vec{R})\psi_\mu(\vec{R}) = E_\mu(R)\psi_\mu(\vec{R}) \quad (1)$$

must be obtained.  $\vec{R}$  is the internuclear separation, and the Hamiltonian  $H(\vec{R})$  includes the electron kinetic energies and all electron-electron, electron-nucleus, and nucleus-nucleus Coulomb interactions. Relativistic effects are not included. All electron coordinates are treated quantum mechanically, but the nuclear coordinates are treated as fixed parameters of  $H(\vec{R})$ .  $H(\vec{R})$  and  $\psi_\mu(\vec{R})$  also depend on all of the electron coordinates, but the notation used here suppresses this dependence. The subscript  $\mu$  represents all symmetry indices and principal quantum numbers necessary to characterize the eigenfunction  $\psi_\mu(\vec{R})$ .

In this calculation, the molecular eigenstates were obtained by the multiconfiguration valence-bond (MCVB) method.<sup>3,4</sup> The set of one-electron atomic orbital basis functions used was identical to the set used in the earlier treatment of the  $\text{Ba}_2^{2+}$  system.<sup>1</sup> As in that calculation, these one-electron functions were used to construct a set of multi-electron functions, which were in turn used as basis vectors in solving Eq. (1). Eigenstates were obtained for the  ${}^2\Sigma_u^+$  and  ${}^2\Sigma_g^+$  molecular symmetries. These symmetries are the only ones that permit the Ba atom and the  $\text{Ba}^+$  ion to both be in their ground states as  $R \rightarrow \infty$ . When the colliding species are in their ground states initially, and if collisional coupling is weak between states of unlike symmetry, then only these two symmetries must be included in the collision dynamics computations.

The one-electron orbitals used in the MCVB calculation consisted of a (7s, 6p, 2d) set centered at each nucleus, for a total of 70 orbitals. Gaussian-type orbitals were used. The numerical values of all scaling factors and coefficients defining the orbitals have been reported previously.<sup>1</sup> As in that previous work, the orbitals at each nucleus were divided into a (5s, 4p, 2d) set of core orbitals and a (2s, 2p) set of valence orbitals. In constructing the multielectron basis functions, every core orbital was required to be doubly occupied in every basis function. All schemes of valence orbital occupation consistent with the molecular symmetry were allowed. A total of 112 basis functions were thus constructed for each symmetry  ${}^2\Sigma_g^+$  and  ${}^2\Sigma_u^+$ . Further details of this MCVB calculation need not be described here, because they do not differ substantially from the details of the previous treatment of the  $\text{Ba}_2^{++}$  system.<sup>1</sup>

The second step in this calculation is to obtain the charge-transfer cross section, by using the previously computed molecular eigenstates as basis vectors for a time-dependent treatment of the colliding system. The impact parameter (IP) version of the perturbed stationary states (PSS) method is used.<sup>5</sup> For clarity, we now state the well-known formulas used in applying this method to the resonant case.

It is assumed that the nuclear motion can be treated classically, and that the nuclear trajectories are straight lines. It is further assumed that the relative nuclear motion is sufficiently slow that the system evolves adiabatically during the collision. Under these conditions, the amplitude for resonant charge transfer is

$$a(v, b) = i \exp[-iS(b)/v] \sin[K(b)/v], \quad (2)$$

where  $v$  and  $b$  are the relative collision speed and impact parameter, respectively, and

$$S(b) = \int_0^\infty [E_g(R') + E_u(R')] dz', \quad (3)$$

$$K(b) = \int_0^\infty [E_g(R') - E_u(R')] dz', \quad (4)$$

$$R'^2 = z'^2 + b^2.$$

The subscripts  $\mu = u$  and  $\mu = g$  denote the states of lowest energy of symmetries  ${}^2\Sigma_u^+$  and  ${}^2\Sigma_g^+$ , respectively. The desired charge-transfer probability is then

$$P(v, b) = \sin^2[K(b)/v], \quad (5)$$

which is the result obtained by Mapleton in his review.<sup>5</sup> The resonant charge-transfer cross section is then, in units of  $\pi a_0^2$ ,

$$\sigma(v) = 2 \int_0^\infty b P(v, b) db. \quad (6)$$

The differential cross section is estimated using a special form of the eikonal method.<sup>6</sup> The amplitude for resonant charge-transfer scattering in a specified direction is simply

$$f(\theta) = Mv \cos^2(\frac{1}{2}\theta) \int_0^\infty b a(v, b) J_0(Mvb \sin\theta) db, \quad (7)$$

where  $\theta$  is the scattering angle,  $M$  is the  $\text{Ba}_2^+$  reduced mass,  $a(v, b)$  is the amplitude of Eq. (2), and  $J_0$  is a Bessel function. The differential cross section is then simply

$$\eta(\theta) = |f(\theta)|^2.$$

Note that this method of estimating the differential cross section does not simply assume that each impact parameter corresponds to a single scattering angle by means of some function  $\theta(b)$ , as is often assumed in classical trajectory treatments of relatively heavy systems.

To summarize, the resonant charge-transfer cross section is computed from the molecular potential energy functions  $E_\mu(R)$  in three simple steps. First, the energy difference integral (4) is computed as a function of  $b$ . Second, the charge-transfer probability is tabulated using Eq. (5). Third, the cross section is obtained as a function of collision speed by computing the integral (6). The differential cross section is computed in two additional steps. First, the energy sum integral (3) is computed as a function of  $b$ . Second, the eikonal integral (7) is computed as a function of scattering angle and collision speed.

### III. NUMERICAL RESULTS

#### A. Molecular eigenstates

The molecular energies  $E_\mu(R)$  for the  ${}^2\Sigma_u^+$  and  ${}^2\Sigma_g^+$  symmetries are presented in Figs. 1 and 2, respectively. The axes in the plots are scaled in atomic units, which are used throughout the remainder of this paper unless otherwise specified.

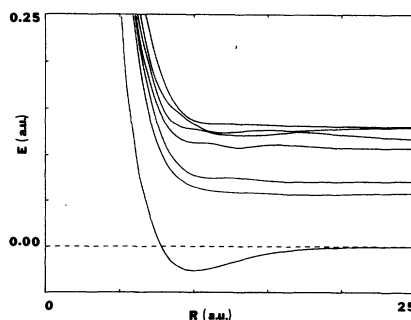


FIG. 1. The  ${}^2\Sigma_u^+$  molecular energies  $E_\mu(R)$  for the  $\text{Ba}_2^+$  system.

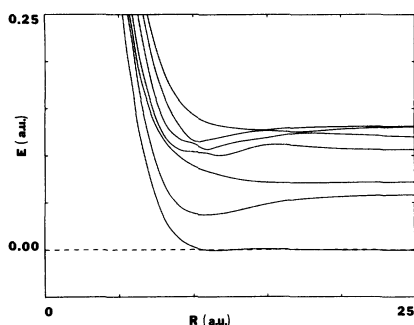


FIG. 2. The  ${}^2\Sigma_g^+$  molecular energies  $E_\mu(R)$  for the  $\text{Ba}_2^+$  system.

The lowest  ${}^2\Sigma_u^+$  curve, of course, exhibits a minimum which demonstrates the presence of significant chemical binding effects in the  $\text{Ba}_2^+$  system. The equilibrium internuclear separation is 10.15, the binding energy is 0.0263, and the vibrational frequency associated with the binding is 0.00024. The  $\text{Ba}_2^+$  binding energy has been experimentally determined to lie between 0.0286 and 0.0350,<sup>7</sup> so that the theoretically determined binding energy is probably in error by at least 10%. To the best of this author's knowledge the equilibrium separation and the vibrational frequency have not yet been experimentally measured.

Somewhat surprisingly, the lowest  ${}^2\Sigma_g^+$  curve also exhibits a minimum. The equilibrium separation, binding energy, and vibrational frequency associated with this minimum are 11.57, 0.00072, and 0.00014, respectively. This apparent binding effect is extremely weak; in units of temperature the stated well depth is only 230 K. It seems likely that the apparent binding is simply a numerical artifact, caused perhaps by the practical necessity of using a very nearly minimal basis in treating a system as large as  $\text{Ba}_2^+$ . If on the other hand the binding is real, then its existence implies the possibility of observing gerade to ungerade electric-dipole transitions in  $\text{Ba}_2^+$ .

The  ${}^2\Sigma_u^+$  and  ${}^2\Sigma_g^+$  ground-state curves cross each other at internuclear separation 3.49. As described in Sec. III B, this crossing has a major effect on the low-energy behavior of the total charge-transfer cross section.

#### B. Charge-transfer collisions

The energy difference

$$D(R) = E_g(R) - E_u(R)$$

and the energy difference integral  $K(b)$  are plotted in Fig. 3. The function  $D(R)$  becomes negative for small  $R$ , because  $E_u(R)$  is greater than  $E_g(R)$  in the extremely repulsive region of the energy curves. This region lies above the upper energy

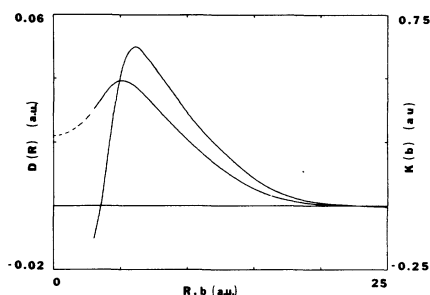


FIG. 3. The energy difference  $D(R)$  and the difference integral  $K(b)$ . The  $D(R)$  curve becomes negative for small  $R$ . The dashed curve represents an extrapolation of  $K(b)$  to  $b=0$ . The abscissa is  $R$  for the  $D(R)$  curve and  $b$  for the  $K(b)$  curve.

limit of Figs. 1 and 2. Let  $R_0$  denote the radius below which  $D(R)$  is negative. The function  $K(b)$  exhibits a local maximum near  $b=R_0$ . This maximum occurs because, as  $b$  decreases below  $R_0$ , the integral (4) receives a progressively larger contribution from the negative portion of the  $D(R)$  curve. Let  $b_0$  denote the impact parameter at which  $K(b)$  is maximum. Note that  $b_0$  and  $R_0$  are not exactly equal.

The dashed curve in Fig. 3 represents an extrapolation of  $K(b)$  from  $b=3$  to  $b=0$ . The extrapolated curve is a second-order polynomial, determined by requiring that  $K(b)$  and its first derivative be continuous at  $b=3$ , and that the derivative be zero at  $b=0$ . This extrapolation is used in estimating the contribution made to the total charge-transfer cross section by small impact parameter collisions.

The charge-transfer probability  $P(v, b)$ , computed from Eq. (5), is plotted in Fig. 4 as a function of impact parameter for six different collision energies  $E$ . The  $E$  values for each plot are, from top to bottom, 400, 170, 80, 35, 27.5, and 17.5, all in keV. The collision speeds associated with these energies are 0.4830, 0.3149, 0.2160, 0.1429, 0.1267, and 0.1010.

The probability curves show an oscillatory behavior similar to that discussed and illustrated by Perel<sup>8</sup> in a treatment of the resonant system  $\text{Li}^+ + \text{Li}$ . In both that system and in the  $\text{Ba}^+ + \text{Ba}$  system, a local extremum in the energy difference integral  $K(b)$  produces a special local extremum in the probability curves, at the impact parameter  $b_0$  for which  $K(b)$  is maximum. At that extremum, the transfer probability oscillates sinusoidally as a function of  $1/v$ , with period

$$\Delta(1/v) = \pi/K_0,$$

where  $K_0 = K(b_0)$  is the maximum value of  $K(b)$ . For the  $\text{Ba}^+ + \text{Ba}$  system,  $b_0 = 5.11$  and  $K_0 = 0.4916$ . The curves in Fig. 4 clearly show the presence

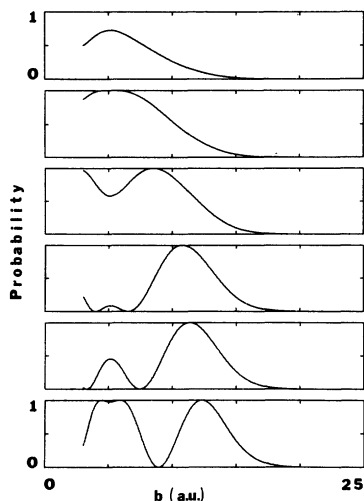


FIG. 4. The charge-transfer probability  $P(v, b)$ , plotted as a function of  $b$  for six energies. From top to bottom these energies are, in keV, 400, 170, 80, 35, 27.5, and 17.5.

of this special local extremum, as do the curves plotted by Perel.<sup>8</sup>

The total charge-transfer cross section  $\sigma(v)$  is plotted in Figs. 5 and 6. In Fig. 5,  $\sigma$  is plotted as a function of collision energy  $E$ , with  $E$  range 0–800 keV. In Fig. 6,  $\sigma$  is plotted as a function of  $1/v$ , with  $1/v$  range 0–40 atomic units. Note that the left-hand and right-hand sides of Fig. 6 correspond to high energies and low energies, respectively.

For most energies included in Fig. 5, the cross section is considerably larger than the geometric cross sections of the Ba and Ba<sup>+</sup> species, because, as shown by Fig. 4, the active electron easily migrates across fairly large internuclear distances during the resonant charge-transfer process. The cross-section curve behaves as  $1/E$  for large

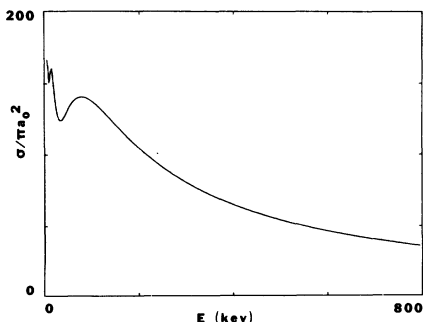


FIG. 5. The charge-transfer cross section  $\sigma(v)$ , plotted as a function of collision energy  $E$ . The contribution due to  $b < 3$  collisions is included, by means of the extrapolated portion of the  $K(b)$  curve in Fig. 3.

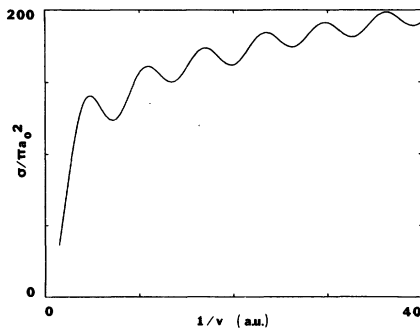


FIG. 6. The charge-transfer cross section  $\sigma(v)$ , plotted as a function of  $1/v$ .

energies; this behavior is well known in resonant charge transfer and is easily deduced from Eqs. (5) and (6). For smaller energies the curve exhibits a rapid oscillatory behavior. Figure 6 shows these oscillations more clearly. The first two maxima on the left side of Fig. 6 corresponds to the two highest-energy maxima visible in Fig. 5. The other maxima in Fig. 6 are not visible in Fig. 5 because they all occur in the narrow energy range to the left of the sharper of the two visible maxima.

The pronounced oscillations in the total cross section are of a type that has been discussed theoretically<sup>9-11</sup> and observed experimentally<sup>12</sup> by a number of authors. These oscillations reflect the oscillation of  $P(v, b)$  at its special extremum at  $b = b_0$ ; these oscillations in  $P$  are so strong that the integration (6) cannot smooth out their effect on the total cross section.

As noted by Olson,<sup>11</sup> these total cross section oscillations are periodic with respect to  $1/v$ . For the Ba<sup>+</sup> + Ba system, their period is

$$\Delta(1/v) = 6.38.$$

An experimental detection of these oscillations, and a measurement of their period, would provide a test of the quality of our Ba<sub>2</sub><sup>+</sup> energy curves calculation.

The differential charge-transfer cross section  $\eta(\theta)$  is plotted in Fig. 7, for collision energy 170 keV. Note that the plot's vertical scale is logarithmic. Because of the Ba<sup>+</sup> + Ba system's great mass the scattering is peaked extremely sharply in the forward direction:  $\eta(\theta)$  falls by nearly three orders of magnitude as  $\theta$  increases from zero to  $0.00002\pi$ . The curve shows an oscillatory structure for very small angles that disappears as the angle increases. Plots (not shown) made for lower energies show that, as the energy decreases, this oscillatory structure smoothly spreads out, increasing its angular width.

The oscillations shown by the  $\eta(\theta)$  curve are not

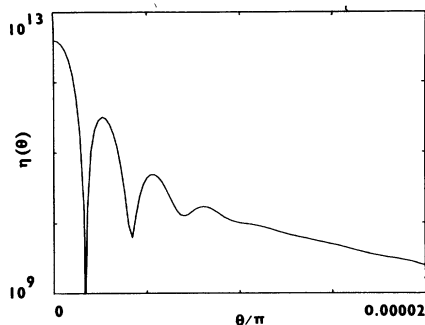


FIG. 7. The differential charge-transfer cross section  $\eta(\theta)$ , in atomic units, plotted as a function of scattering angle  $\theta$  for collision energy 170 keV. The plot's vertical scale is logarithmic.

related to the oscillations, previously discussed, shown by the  $P(v, b)$  curves (Fig. 4). The  $\eta(\theta)$  oscillations reflect the oscillatory behavior of the Bessel function factor  $J_0$  in the integrand of Eq. (7). Physically, these oscillations are simply diffraction fringes due to interference between collisions occurring at different impact parameters. The  $P(v, b)$  oscillations are totally masked by the integration (7) and therefore do not affect the differential cross section's basic structure. The  $\eta(\theta)$  oscillations are in principle observable, although of course it would be impractical to build an apparatus capable of doing so. The chief conclusion of the differential cross section calculation is that, despite the great mass of the colliding ions and their extremely short deBroglie wavelengths, each impact parameter  $b$  cannot be assumed to correspond to a single scattering angle  $\theta$ . Although the classical trajectory model of the nuclear motion is probably valid in predicting total cross sections, it is not valid in predicting differential cross sections.

#### IV. DISCUSSION

We now compare the results of the present calculation with the results of the previous treatment of the nonresonant  $\text{Ba}^+ + \text{Ba}^+ \rightarrow \text{Ba} + \text{Ba}^{2+}$  collision.<sup>1</sup> Because the resonant and nonresonant heavy ion charge-transfer processes are dominated by fundamentally different physical mechanisms, the results of the two calculations differ drastically in their major qualitative features. The major features of the previous results illustrated the domination of nonresonant charge transfer by collisional coupling between a ground state and excited states of like molecular symmetry. The present results illustrate the domination of resonant charge-transfer by coupling between ground states of unlike molecular symmetry.

Because resonant charge transfer does not require coupling to excited states, the cross section remains large for small collision energies (Fig. 5). Because coupling to excited states becomes vanishingly weak for low collision speeds and because nonresonant charge transfer does require such coupling, the nonresonant cross section is large only for collision energies of several hundred keV; the cross section becomes small for low energies. The results of the previous calculation<sup>1</sup> clearly illustrate this behavior.

The previous calculation showed that, for the  $\text{Ba}^+ + \text{Ba}^+$  system, the presence or absence of avoided crossings in the system's molecular energy curves greatly affects the nonresonant charge-transfer process. Significant nonresonant transfer was predicted, for large impact parameter collisions, only for molecular symmetries for which avoided crossings between the ground state and the first excited state curves occurred at large internuclear distances. The present calculation shows that, for the  $\text{Ba}^+ + \text{Ba}$  system, significant resonant charge transfer occurs for large impact parameters even when no avoided energy-curve crossings involving the ground state are present. Resonant and nonresonant charge transfer processes in general should differ from each other in this same way.

The present calculation shows that the structural details of the impact-parameter-dependent charge-transfer probability are not physically observable in the differential cross section, for the resonant system. Although no differential cross sections were computed in the earlier work, it is reasonable to expect that the same is true for nonresonant systems, provided that the colliding species are not very highly ionized. In collisions between highly ionized species, the angular deflections involved may be sufficiently large that an approximation associating each impact parameter with a single scattering angle may be reasonable. In such cases, the structural details of the impact-parameter-dependent probability would be observable in the differential cross section.

#### ACKNOWLEDGMENT

The author wishes to thank Professor Joseph H. Macek and Professor Gordon A. Gallup for helpful discussions and suggestions. The MCVB molecular quantum mechanics computer codes were developed in Professor Gallup's laboratory. Mr. Robert L. Vance rendered valuable assistance in using these codes. This research was supported by the United States Department of Energy, Contract No. EG-77-S-02-4379.

- <sup>1</sup>Stanley J. Sramek, G. A. Gallup, and J. H. Macek, Phys. Rev. A (in press).
- <sup>2</sup>Proceedings of the Heavy Ion Fusion Workshop, Argonne National Laboratory, September 19–26, 1978, available from National Technical Information Service, U. S. Dept. of Commerce, 528 Port Royal Road, Springfield, Va.
- <sup>3</sup>G. A. Gallup, Int. J. Quantum Chem. VI, 761–777 (1972).
- <sup>4</sup>G. A. Gallup, Int. J. Quantum Chem. VI, 899–909 (1972).
- <sup>5</sup>Robert A. Mapleton, *Theory of Charge Exchange* (Wiley, N. Y., 1972), pp. 30–36.
- <sup>6</sup>L. Wilets and S. J. Wallace, Phys. Rev. 169, 84 (1968).
- <sup>7</sup>Earl F. Worden, Jeffrey A. Paisner, and John G. Conway, abstract of paper presented at *The Symposium on Atomic Spectroscopy*, Tucson, Arizona, September 10–14, 1979 (unpublished).
- <sup>8</sup>Julius Perel, Phys. Rev. A 1, 369 (1970).
- <sup>9</sup>F. J. Smith, Phys. Lett. 20, 271 (1966).
- <sup>10</sup>J. M. Peek, T. A. Green, J. Perel, and H. H. Michels, Phys. Rev. Lett. 20, 1419 (1968).
- <sup>11</sup>R. E. Olson, Phys. Rev. 187, 153 (1969).
- <sup>12</sup>For an extensive experimental bibliography, see R. E. Olson, Phys. Rev. A 2, 121 (1970).